The origin of the conformational change can be further explored by the technique of site-directed spin labeling, in which nitroxide spin labels are selectively placed through the use of site-directed mutagenesis. With a set of spin-labeled proteins, this strategy can provide both secondary and tertiary structural information (*28*) and should permit a detailed interpretation of the conformational change observed here. The feasibility of such studies has recently been demonstrated for rhodopsin (*29*). This approach should be particularly useful for other receptors that have no natural chromophore as an indirect indicator of structural changes.

REFERENCES AND NOTES

1. T. E. Thorgeirsson, J. W. Lewis, S. E. Wallace-Williams, D. S. Kliger, *Photochem. Photobiol.* **56**, 1135 (1992).
2. K. P. Hofmann, *Photochem. Photobiophys.* **13**, 309 (1986).
3. H. Kuhn, O. Mommertz, P. A. Hargrave, *Biochim. Biophys. Acta* **679**, 95 (1982).
4. W. J. DeGrip *et al.*, *Photochem. Photobiol.* **48**, 497 (1988); U. M. Ganter, T. Charitopoulosw, N. Virmaux, F. Siebert, *ibid.* **56**, 57 (1992); A. K. Klinger and M. S. Braiman, *Biophys. J.* **63**, 1244 (1992).
5. M. Chabre, *Proc. Natl. Acad. Sci. U.S.A.* **75**, 5471 (1978); C. N. Rafferty, J. Y. Cassim, D. G. McConnell, *Biophys. Struct. Mech.* **2**, 227 (1977).
6. C. Pellicone, N. J. Cook, G. Nullans, N. Virmaux, *FEBS Lett.* **184**, 179 (1985).
7. M. Chabre, *Annu. Rev. Biophys. Chem.* **14**, 331 (1985).
8. G. F. X. Schertler, C. Villa, R. Henderson, *Nature* **362**, 770 (1993).
9. E. A. Dratz and P. A. Hargrave, *Trends Biochem. Sci.* **8**, 128 (1983).
10. J. B. C. Findlay *et al.*, *Vision Res.* **24**, 1501 (1984).
11. H. G. Khorana, *J. Biol. Chem.* **267**, 1 (1992).
12. Y. S. Chen and W. L. Hubbell, *Membr. Biochem.* **1**, 107 (1978).
13. K. P. Hofmann and J. Reichert, *J. Biol. Chem.* **260**, 7990 (1985).
14. S. Ogawa and H. M. McConnell, *Proc. Natl. Acad. Sci. U.S.A.* **58**, 19 (1967); J. K. Moffat, *J. Mol. Biol.* **55**, 135 (1971).
15. To determine the topographical location of the spin-labeled site in the molecule, the accessibility of the nitroxide to collision with CrOx and O_2 has been measured according to Farahbakhsh and colleagues [*Photochem. Photobiol.* **56**, 1019 (1992)]. The accessibility expressed as a dimensionless π value is 0.6 and 0.2 for O_2 and CrOx, respectively. These values correspond to those for solvent-exposed residues. There was no change in π after photoexcitation.
16. K. Hideg *et al.*, unpublished results.
17. Z. T. Farahbakhsh, C. Altenbach, W. L. Hubbell, *Photochem. Photobiol.* **56**, 1019 (1992).
18. M. Delmelle and N. Virmaux, *Biochim. Biophys. Acta* **464**, 370 (1977).
19. J. Kibelbek, D. C. Mitchell, J. M. Beach, B. J. Litman, *Biochemistry* **30**, 6761 (1991).
20. K. J. Rothschild, J. Gillespie, W. J. DeGrip, *Biophys. J.* **51**, 345 (1987).
21. R. R. Franke, B. König, T. P. Sakmar, H. G. Khorana, K. P. Hofmann, *Science* **250**, 123 (1990).
22. B. König *et al.*, *Proc. Natl. Acad. Sci.* **86**, 6878 (1989).
23. C. Chothia and A. M. Lesk, *Trends Biochem. Sci.* **114**, 116 (1985); C. A. McPhalen *et al.*, *J. Mol. Biol.* **227**, 197 (1992); S. Subramaniam, M. Gerstein, D. Oesterhelt, R. Henderson, *EMBO J.* **12**, 1 (1993).
24. T. P. Sakmar, R. R. Franke, H. G. Khorana, *Proc. Natl. Acad. Sci. U.S.A.* **86**, 8309 (1989); E. A. Zhukovsky and D. D. Oprian, *Science* **246**, 928 (1989).
25. E. A. Zhukovsky, P. R. Robinson, D. D. Oprian, *Biochemistry* **31**, 10400 (1992).
26. P. R. Robinson, G. B. Cohen, E. A. Zhukovsky, D. D. Oprian, *Neuron* **9**, 719 (1992); G. B. Cohen, T. Yang, P. R. Robinson, D. D. Oprian, *Biochemistry* **32**, 6111 (1993).
27. J. M. Baldwin, *EMBO J.* **12**, 1693 (1993).
28. C. Altenbach, T. Marti, H. G. Khorana, W. L. Hubbell, *Science* **248**, 1088 (1990).
29. J. Resek, Z. T. Farahbakhsh, W. L. Hubbell, H. G. Khorana, *Biochemistry*, in press.
30. Abbreviations for the amino acid residues are as follows: A, Ala; C, Cys; D, Asp; E, Glu; F, Phe; G, Gly; H, His; I, Ile; K, Lys; L, Leu; M, Met; N, Asn; P, Pro; Q, Gln; R, Arg; S, Ser; T, Thr; V, Val; W, Trp; and Y, Tyr.

31. Supported by NIH grant EY05216, NIH training grant EY07026, Hungarian Research Foundation grant OTKA/3/42, and the Jules Stein Professor Endowment.

15 July 1993; accepted 1 October 1993

Nonlinear Optical Properties of Proteins Measured by Hyper-Rayleigh Scattering in Solution

K. Clays, E. Hendrickx, M. Triest, T. Verbiest, A. Persoons,* C. Dehu, J.-L. Brédas

Hyper-Rayleigh scattering has been used to determine the nonlinear optical properties of a chromophore-containing protein in solution. Because the technique of hyper-Rayleigh scattering allows the measurement of hyperpolarizabilities in an isotropic solution without the application of an electric field, this method is ideally suited for the study of proteins that carry a net charge. The observed orientational correlation between the nonlinear optical chromophores in incompletely solubilized protein molecules suggests that guidelines from protein structures can be used for the engineering of supramolecular structures with high optical nonlinearity.

The light-energy–transducing protein bacteriorhodopsin (bR) has received considerable attention for potential application in molecular opto-electronic devices (*1–5*). The protein is present in the purple membrane (PM) of halophilic bacteria (*6, 7*). Energy production in these bacteria is based on a proton gradient established by light absorption. The light-driven proton pump action of bR is due to the retinal chromophore, which is bound to the ϵ amino group of the lysine-216 amino acid residue of the protein to form the retinylidene-*n*-butylamine Schiff base. Upon photoexcitation, the proton of the protonated Schiff base is released and follows a channel of hydrogen bonds toward the cellular exterior.

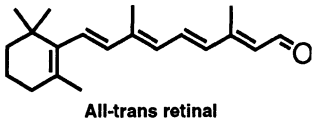

All-trans retinal

The conjugated chain in the retinal chromophore permits large odd-order electronic polarizabilities along the chain direction. In addition, the overall molecular symmetry allows second-order nonlinear optical effects. Because of the symmetry restrictions for even-order nonlinear optical effects, the direct determination of the second-order polarizability, first hyperpolarizability β, in the series expansion of the dipole moment μ_i induced by application of a strong electric field E

$$\mu_i = \alpha_{ij} \cdot E_j + \beta_{ijk} \cdot E_j E_k + \gamma_{ijkl} \cdot E_j E_k E_l + \ldots$$

can only be performed in macroscopically noncentrosymmetric ensembles. The classical experimental technique for the determination of the first hyperpolarizability of polar molecules in solution, electric-field–induced second-harmonic generation (EFISHG) (*8–10*), makes use of a dc electric field to orient the dipolar molecules. A temperature-dependent orienting of the molecules in the field then allows frequency-doubling of an intense laser pulse. Because the efficiency of frequency-doubling is dependent on the degree of dipolar orientation, the net result from an EFISHG measurement is the scalar product $\mu\beta$ of the permanent dipole moment vector μ with the vector part of the first hyperpolarizability β. Thus, the value of the dipole moment is necessary to deduce a value for β. Another possible source of error in EFISHG is the estimation of the local field factor, which accounts for the difference between the amplitude of the externally applied electric field and the actual field experienced by the molecule.

However, the EFISHG technique cannot be used with conducting solutions; thus, it cannot probe ionic materials that

K. Clays, E. Hendrickx, M. Triest, T. Verbiest, A. Persoons, Laboratory of Chemical and Biological Dynamics, Center for Research on Molecular Electronics and Photonics, University of Leuven, Celestijnenlaan 200D, B-3001 Leuven, Belgium.

C. Dehu and J.-L. Brédas, Service de Chimie des Matériaux Nouveaux, Centre de Recherche en Electronique et Photonique Moléculaire, Université de Mons-Hainaut, B-7000 Mons, Belgium.

*To whom correspondence should be addressed.

might have a large nonlinear optical (NLO) response. Inasmuch as a reasonable electric field can be established over a conducting solution, the field will cause migration of the ionic species rather than dipolar orientation. Even at the isoelectric point of proteins, when there is no net charge and hence no migration, the orientation of the protein in the field is determined by the location of the charged amino acid residues rather than by the static dipole moment of the chromophore in the protein. This determination explains why the first hyperpolarizability of bR has only been determined experimentally in oriented poly(vinyl alcohol) (PVA) matrices (*11*). A large uncertainty then arises from the estimation of the chromophore orientation angle because of the assumption of a narrow distribution of tilt angles.

Another, indirect technique that has been used to measure the first hyperpolarizability of a protein, without the need for an orienting field, is based on the two-photon absorptivity of a low-lying strongly allowed state (*12, 13*). This technique is based on the reduction of a third-order process (two-photon absorption) to a second-order process (second-harmonic generation) under near resonance conditions. The derived value for β is, however, dependent on the choice of the electronic transition bandwidth.

The technique of hyper-Rayleigh scattering (HRS) in solution (*14–16*) can determine the first hyperpolarizability without an applied orienting electric field and is, therefore, also applicable to ionic media (*17, 18*). This method has been used to measure the first hyperpolarizability of apolar ionic molecules (*18*) and mixed-valence, metal complex chromophores (*17*). Here we have applied the HRS technique to the study of the nonlinear optical properties of bR and the retinal chromophore. The pulsed laser source is an injection-seeded Nd:YAG laser. The fundamental light (1064 nm) is focused into a small cuvette. We checked the quadratic dependence of the intensity of the frequency-doubled scattered light on the fundamental light intensity by varying the latter by means of a half-wave plate between two polarizers. The harmonic light is collected with an efficient photon condensing system and filtered from the fundamental, linearly scattered light. The intensity of the fundamental light, measured with a fast photodiode, and the intensity of the scattered light, detected with a sensitive photomultiplier, are measured by gated integrators (*15, 16*). The determination of the molecular first hyperpolarizability by HRS relies on orientational fluctuations in an isotropic solution (*16*). The intensity of the scattered light at the harmonic frequency is related to the square of the hyperpolarizability of all

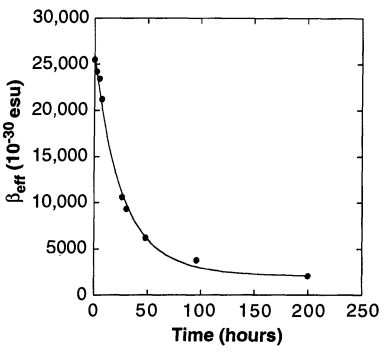

Fig. 1. Time dependence of the effective first hyperpolarizability due to solubilization. The solid trace is a fit to the equation $\beta_{eff} = \beta_{bR}(1 + n \exp -t/\tau)^2$ that is valid in the case of coherent second-harmonic scattering from n exp $- t/\tau$ correlated scatterers.

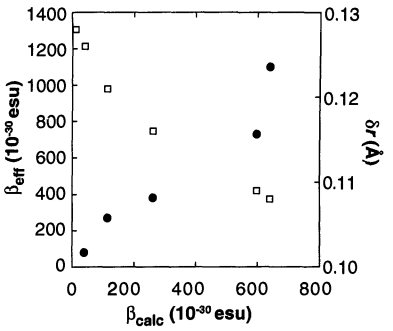

Fig. 2. Correlation between experimental (1064 nm) and calculated (static) first hyperpolarizabilities (filled circles) and between bond-length alternation and calculated hyperpolarizability (open squares) for all-trans retinal in different solvents.

species present in solution. Because of the low nonlinearity of water and the large β_{eff} of bR, the HRS signal $S(2\omega)$ can be effectively approximated by

$$S(2\omega) = GN_{bR}\beta_{eff}^2$$

where G is a proportionality constant containing theoretical, geometrical, and electronic factors, and N_{bR} is the number density of bR molecules in solution. Because there is no measurable signal from the solvent, the internal reference method could not be applied. The appropriate local field correction factors were then applied for the external reference with *para*-nitroaniline in methanol [$\beta = 34.5 \times 10^{-30}$ electrostatic units (esu)]. When the NLO chromophore is absorbing, as is the case with a visual pigment, the HRS signal as a function of chromophore concentration is also determined by the extinction coefficient (*19*).

The bR was solubilized in Triton X-100 (5% v/v) in an acetate buffer (0.1 M, pH 5.0). This solubilization ultimately results in one monomer of bR protein solubilized by one micelle of Triton X-100 (*20*). The kinetics of the solubilization process have been studied in detail (*21*). We have also been able to follow the solubilization of bR (at a number density $N_{bR} = 1.25 \times 10^{15}$ cm^{-3}) from oligomers to monomers with HRS because the intensity of the frequency-doubled light scales as the square of the number of correlated scattering species.

The retrieved effective first hyperpolarizability β_{eff} as a function of time t is shown in Fig. 1. The solid line is a fit to the equation $\beta_{eff} = \beta_{bR}$ $(1 + n \exp -t/\tau)^2$. When the solubilization is incomplete, bR is present as a mixture of trimers, dimers, and monomers, represented by the factor $(1 + n \exp -t/\tau)$. The factor n thus represents the initial degree of association. The presence of bR contributes to the nonlinear scattered light that decays to 1 as the solubilization reaches completion. The relaxation time for solubilization τ of 37 hours, as determined by correlated HRS, is in good agreement with the time constant for solubilization obtained from quasi-elastic (linear) light scattering. The particle diameter decreased according to the equation $d_{eff} = d_{bR,sol} + c \exp -t/\tau$, with τ of 36 hours. The factor c represents the additional volume of the particle corresponding to the initial degree of association n. The particle diameter after complete solubilization [$d_{eff}(\infty) = d_{bR,sol} = 11.5$ nm] compares favorably with published values for the hydrodynamic radius of bR solubilized in Triton X-100 (5.5 nm) (*22, 23*).

The value for β_{eff} after complete solubilization is $\beta_{eff}(\infty) = \beta_{bR} = (2100 \pm 100) \times 10^{-30}$ esu. This value is enhanced by two-photon resonance due to the absorption maximum of bR at 570 nm and is in good agreement with the value determined indirectly from two-photon absorption spectroscopy under near resonance conditions, on the assumption of a damping constant equal to the homogeneous line width of $(2250 \pm 240) \times 10^{-30}$ esu (*12, 13*). It is also in agreement with the value obtained from second-harmonic generation (SHG) in PM-PVA films, on the assumption of a 30° angle between the polyene chain of the retinal chromophore and the normal to the plane of the film of 2500×10^{-30} esu (*11*). The HRS value, determined directly from the intensity of the nonlinear scattered light after complete solubilization, does not depend on assumed values for damping constants or orientation angle and is therefore more accurate than the EFISHG value. The nonlinear scattering experiment (a second-order experiment on an isotropic sample) is much easier to perform than two-photon absorption spectroscopy (a third-order, nonlinear optical experiment on an isotropic sample) or SHG on PM-PVA films (a second-order technique but on a

Table 1. Comparison, as a function of solvent, between experimental effective second-order polarizabilities β_{eff} (1064 nm) for all-trans retinal and the calculated static values β_{calc} for the conjugated part of the molecule. The calculated optimal δr values and dielectric constants ϵ are also provided.

Solvent	β_{eff} (10^{-30} esu)	β_{calc} (10^{-30} esu)	δ (Å)	ϵ
Gas phase		11.5	0.128	1
Dioxane	80	39.6	0.126	2.2
Chloroform	270	113	0.121	4.81
Dichloroethane	380	261	0.116	10.6
Methanol	730	598	0.109	32.63
Nitromethane	1100	641	0.108	35.9

non-centrosymmetric sample).

The retrieved β value of 2100×10^{-30} esu for bR should be compared with the β value of 450×10^{-30} esu for the well-known 4-*N*,*N*-dimethylamino-4′-nitrostilbene molecule (*24*, *25*). While the β value found for bR is large, the correlated scattering from molecules suggests that interaction between (modified) protein molecules can be used to stabilize the trimeric form to enhance the macroscopic susceptibility by a factor of 10, as shown in Fig. 1 at time 0.

The second-order NLO response of bR stems from the retinal chromophore that is Schiff-bonded to the lysine-216 amino acid residue (*6*). We have therefore also studied the NLO properties of all-trans retinal, which is the actual chromophore in bR. The EFISHG technique has been used to study retinal in dimethyl sulfoxide (*26*). Our values for β of retinal in different solvents are consistently higher than those derived from the reported value of 230×10^{-48} esu for $\mu\beta$. Because of its long conjugated chain in the all-trans configuration, retinal has a large third-order polarizability γ (*27*). According to the internal reaction field theory, the solvent dependence of the effective second-order polarizability can be explained in terms of the solvent-parameter density, molecular weight, refractive index and dielectric constant, and the dipole moment and third-order hyperpolarizability of the NLO chromophore (*16*). The experimental value for β_{eff} is independent of the measurement technique used (HRS or EFISHG). However, with EFISHG a knowledge of the dipole moment and the second hyperpolarizability is necessary to retrieve a value for β_{eff}. On the basis of internal reaction field theory, the large third-order polarizability γ of all-trans retinal (*27*), together with the ground-state dipole moment of 5.3 D (*28*), should cause a large solvent dependence. This dependence has been observed experimentally for the retinal chromophore (Table 1).

We have performed quantum chemical calculations on the static β response at the Hartree-Fock ab initio level using a split-valence (3- to 21-G) basis set. Such a theoretical approach has been found to provide excellent trends in comparison to experimental data in the case of donor-acceptor polyenes (*29*). Furthermore, we have explicitly taken into account the influence of solvent by following Onsager's self-consistent reaction field approach (*30*), as implemented in the Gaussian-92 set of programs (*31*). In this model, the solute is considered to occupy a spherical cavity within a continuous medium of dielectric constant ϵ. The geometry of the molecule is fully optimized, and the molecular second-order polarizability was evaluated, through the coupled perturbed Hartree-Fock scheme (*32*, *33*), in the presence of the appropriate dielectric. As the polarity increases, the average degree of bond-length alternation δr (the average value of the difference between adjacent carbon-carbon double and single bonds along the retinal conjugated backbone) decreases slightly as β increases. This relation is in line with what has been observed by Marder and colleagues in the case of donor-acceptor polyenes (*34*–*36*). In Table 1 we report the values for optimized δr, together with those for calculated static β, and for β measured at 1064 nm. There is only a small shift of the wavelength of the absorption maximum from 380 to 390 nm upon the change from apolar to polar solvents.

Solvent polarity exerts a major influence on the second-order nonlinear optical response. The static hyperpolarizability is calculated to grow by a factor of 4 in moving from the gas phase ($\beta = 11.5 \times 10^{-30}$ esu; $\epsilon = 1$) to dioxane ($\beta = 39.6 \times 10^{-30}$ esu; $\epsilon = 2.2$) and by another factor of 15 from dioxane to nitromethane ($\beta = 640.6 \times 10^{-30}$ esu; $\epsilon = 35.9$). This 15-fold increase is in good agreement with the experimentally measured value of β by a factor of ~13.5 from dioxane [β (1064 nm) = 80×10^{-30} esu] to nitromethane [β (1064 nm) = 1100×10^{-30} esu]. The correlation between theory and experiment is illustrated in Fig. 2.

An exception is found in the case of methanol, in which the low measured β value could originate from hydrogen bond formation. The theoretical values are about twice as small as the experimental values; this feature is due to the neglect in the calculations of the effects related to electron correlation (*37*) and frequency dispersion. Both types of effects increase the value of β. The 60-fold increase in the calculated static β value between the dielectric media with $\epsilon = 1$ (gas phase) and $\epsilon = 35.9$ (simulating nitromethane) is significantly larger than what has been calculated by Marder and co-workers (*34*–*36*) for donor-acceptor polyenes at a comparable level of evolution of the degree of bond-length alternation. We are now evaluating, through a sum-over-states approach, the physical origin of such a strong increase.

We can determine the first hyperpolarizability of a chromophore-containing protein with good accuracy by means of an experimentally simple technique, HRS. The observed solvent dependence of β of the isolated chromophore can be explained in terms of the internal reaction field of the solution. The results of self-consistent reaction-field theory show a good correlation with the experimental results. The correlations between chromophores embedded in interacting protein molecules have a large influence on their effective first hyperpolarizability (Fig. 1). This relation suggests that guidelines derived from protein structures can be used for the engineering of supramolecular structures with very high optical nonlinearities.

REFERENCES AND NOTES

1. D. Oesterhelt, C. Braüchle, N. Hampp, *Q. Rev. Biophys.* **24**, 425 (1991).
2. C. Braüchle, N. Hampp, D. Oesterhelt, *Adv. Mater.* **3**, 420 (1991).
3. C. Braüchle, *Appl. Opt.* **31**, 1834 (1992).
4. T. Miyasaka, K. Koyama, I. Itoh, *Science* **255**, 342 (1992).
5. Q. W. Song, C. Zhang, R. Gross, R. Birge, *Opt. Lett.* **18**, 775 (1993).
6. W. Stoeckenius and R. A. Bogomolni, *Annu. Rev. Biochem.* **52**, 587 (1982).
7. R. B. Birge, *Biochim. Biophys. Acta* **1016**, 293 (1990).
8. B. F. Levine and C. G. Bethea, *J. Chem. Phys.* **63**, 2666 (1975).
9. K. D. Singer and A. F. Garito, *ibid.* **75**, 3572 (1981).
10. G. R. Meredith, *Rev. Sci. Instrum.* **53**, 48 (1982).
11. J. Y. Huang, Z. Chen, A. Lewis, *J. Phys. Chem.* **93**, 3314 (1989).
12. R. R. Birge and C.-F. Zhang, *J. Chem. Phys.* **92**, 7178 (1990).
13. R. R. Birge, P. A. Fleitz, A. F. Lawrence, M. A. Masthay, C. F. Zhang, *Mol. Cryst. Liq. Cryst.* **189**, 107 (1990).
14. K. Clays and A. Persoons, *Phys. Rev. Lett.* **66**, 2980 (1991).
15. ———, *Rev. Sci. Instrum.* **63**, 3285 (1992).
16. ———, L. D. Maeyer, *Adv. Chem. Phys.* **85B**, 455 (1993).
17. W. M. Laidlaw, R. G. Denning, T. Verbiest, E. Chauchard, A. Persoons, *Nature* **363**, 58 (1993).
18. T. Verbiest, K. Clays, A. Persoons, F. Meyers, J.-L. Brédas, *Opt. Lett.* **18**, 525 (1993).
19. T. Verbiest, E. Hendrickx, A. Persoons, K. Clays, *Proc. Soc. Photo-Opt. Instrum. Eng.* **1775**, 206 (1993).
20. J. A. Reynolds and W. Stoeckenius, *Proc. Natl. Acad. Sci. U.S.A.* **74**, 2803 (1977).
21. N. A. Dencher and M. P. Heyn, *FEBS Lett.* **96**, 322 (1978).

22. H. B. Osborne, C. Sardet, A. Helenius, *Eur. J. Biochem.* **44**, 383 (1974).
23. M. Seigneuret, J.-M. Neumann, J.-L. Rigaud, *J. Biol. Chem.* **266**, 10066 (1991).
24. J. L. Oudar and H. L. Person, *Opt. Commun.* **15**, 258 (1976).
25. J. L. Oudar, *J. Chem. Phys.* **67**, 446 (1977).
26. Y. Kawabe, H. Ikeda, T. Sakai, K. Kawasaki, *J. Mater. Chem.* **2**, 1025 (1992).
27. J. P. Hermann and J. Ducuing, *J. Appl. Phys.* **45**, 5100 (1974).
28. M. Ponder and R. Mathies, *J. Phys. Chem.* **87**, 5090 (1983).
29. F. Meyers, J.-L. Brédas, J. Zyss, *J. Am. Chem. Soc.* **114**, 2914 (1992).
30. L. Onsager, *ibid.* **58**, 1486 (1936).
31. M. W. Wong, K. B. Wiberg, M. J. Frisch, *ibid.* **115**, 1078 (1993).
32. C. E. Dykstra and P. G. Jasien, *Chem. Phys. Lett.* **109**, 388 (1984).
33. G. J. B. Hurst, M. Dupuis, E. Clementi, *J. Chem. Phys.* **89**, 385 (1988).
34. S. R. Marder, C. B. Gorman, L.-T. Cheng, B. G. Tiemann, *Proc. Soc. Photo-Opt. Instrum. Eng.* **1775**, 19 (1993).
35. C. B. Gorman and S. R. Marder, *Proc. Natl. Acad. Sci. U.S.A.*, in press.
36. S. R. Marder *et al.*, *J. Am. Chem. Soc.* **115**, 2524 (1993).
37. F. Simm, S. Chin, M. Dupuis, J. E. Rice, *J. Phys. Chem.* **97**, 1158 (1993).
38. We dedicate this report to Leo De Maeyer on the occasion of his retirement. Supported by the Belgian National Fund for Scientific Research (FNRS/NFWO) (E.H. and K.C.), the Belgian Prime Minister Office of Science Policy under the Interuniversity Attraction Pole on Supramolecular Chemistry and Catalysis, and the Impulse Program on Information Technology (IT/SC/22).

28 June 1993; accepted 7 September 1993

Single Molecules Observed by Near-Field Scanning Optical Microscopy

Eric Betzig and Robert J. Chichester

Individual carbocyanine dye molecules in a sub-monolayer spread have been imaged with near-field scanning optical microscopy. Molecules can be repeatedly detected and spatially localized (to ~λ/50 where λ is the wavelength of light) with a sensitivity of at least 0.005 molecules/(Hz)$^{1/2}$ and the orientation of each molecular dipole can be determined. This information is exploited to map the electric field distribution in the near-field aperture with molecular spatial resolution.

Emerging techniques aimed at single molecule detection (SMD) have potential applications across the physical sciences. SMD represents the ultimate goal in trace chemical analysis (*1*) and has been proposed as a tool for rapid base-sequencing of DNA (*2, 3*). SMD of site-specific fluorescent probes attached to, for example, individual membrane bound proteins would permit the investigation of such systems with minimal perturbations introduced by the labeling process and without the averaging of physical properties (such as dipole orientations or spectra) associated with the sampling of larger populations. Furthermore, the sensitivity of such properties to environmental conditions could be exploited to locally probe the immediate surroundings of each individual molecule (*4, 5*). Finally, SMD would facilitate fundamental studies of the process of fluorescence emission, including the probability of photobleaching and variations in both the excited state lifetime (*6*) and the angular distribution of emitted radiation which can occur in the vicinity of a dielectric interface (*7–9*).

Although SMD of molecules with numerous (~30) chromophores has been possible for some time (*10–12*), it is only recently that two different approaches have been developed for the detection of single chromophore dyes which are of greatest interest for the above applications. The first involves spectral isolation at low temperature (~1.5 K) of a single absorption (*4*) or fluorescence excitation (*5*) peak in the wings of an inhomogeneously broadened line. Of more general applicability are efforts involving SMD in solution, where the central problem of isolating the molecular fluorescence signal from background luminescence and Raman scattering is overcome by reducing the excitation volume to the smallest possible size, either with levitated microdroplets (*1*) or within a thin flow cell (*3*). Remaining problems with these latter methods include a low measurement bandwidth, photobleaching of the molecule in the course of detection, and a limited degree of confidence in each potential detection event.

To achieve further gains in SMD, we have reduced the optical excitation volume even further—indeed, to subwavelength proportions in all three dimensions. This is accomplished using illumination mode near-field scanning optical microscopy (NSOM) (*13*). In this technique, visible light is funneled through a small aperture (100 nm in these experiments) at the end of a sharp and otherwise opaque probe (*14*) to transversely illuminate at most an aperture sized region of the sample at any one time. Confinement of the detection volume in the axial direction is achieved with a photon-counting avalanche photodiode (APD) of small active area (100 μm), high quantum efficiency (55% at 630 nm), and low dark noise (seven counts per second) which is confocal with the aperture in the image plane of the far-field objective used to collect the fluorescence emission from individual molecules (*15*). Further axial confinement of this signal may be afforded by enhanced fluorescence excitation from evanescent fields of large amplitude predicted to exist in the near field of a subwavelength aperture (*16*). Complete images of the lateral distribution of molecules with transverse resolution on the order of the aperture size can then be generated by raster scanning the sample relative to the probe and recording the fluorescence signal obtained at each point (*17*).

As an initial test of this approach to SMD, a sample was prepared by spreading a dilute methanol solution of the lipophilic carbocyanine dye diIC$_{12}$(3) (Molecular Probes #D-383) across a cover slip previously spin coated with an ~30-nm-thick polymethylmethacrylate (PMMA) film to achieve a *calculated* areal density of ~23 molecules μm^{-2} (*18*). DiIC$_{12}$(3) was chosen for its photostability, large absorption cross section, and significance as a membrane probe (*19*). PMMA was used because it was empirically observed to enhance both the apparent quantum yield and adhesion of the individual molecules. The sample was then imaged with the NSOM system described in (*13*) and (*15*), with the results shown in Fig. 1 as six images (*20*) of the same region obtained sequentially but under differing polarization conditions.

A wealth of information can be extracted from this data. We begin with the evidence that the individual structures observed represent luminescence from single molecules. The arguments are fivefold. First, the areal density of ~3.5 molecules μm^{-2} measured from Fig. 1A is only about a factor of 6 lower than that calculated above, with the discrepancy probably attributable to considerable unevenness in the spreading process, photobleaching in the original solution or on the substrate, and nonradiative energy transfer from certain molecules in unfavorable local environments. Second, the density changes linearly over almost three orders of magnitude with changes in the concentration of the solution. Third, the peak signal observed (for example, 380 counts in 10 ms for molecule b in Fig. 1D) is consistent with the emission expected from a single diIC$_{12}$(3) molecule under the known excitation conditions (*21*). Fourth, each structure in Fig. 1 has a well-defined dipole orientation as discussed below. Finally,

AT&T Bell Laboratories, 600 Mountain Avenue, Murray Hill, NJ 07974.